Journal of Molecular Structure 1154 (2018) 373–381

Contents lists available at ScienceDirect

Journal of Molecular Structure

journal homepage: http://www.elsevier.com/locate/molstruc

Anagostic interactions in chiral separation. Polymorphism in a [Co(II)(L)] complex: Crystallographic and theoretical studies

Firas F. Awwadi*, Hamdallah A. Hodali

Department of Chemistry, The University of Jordan, Amman 11942, Jordan

ARTICLE INFO

Article history:
Received 21 June 2017
Received in revised form
19 October 2017
Accepted 19 October 2017
Available online 20 October 2017

Keywords:
Chiral separation
Polymorphism
cis-1,2-Disubstituted cyclohexane conformers
Anagostic interactions
Conformation analysis
DFT calculations

ABSTRACT

Syntheses and crystal structures of two polymorphs of the complex [Co(II)(L)], where H_2L = 2,2'-[*cis*-1,2-diaminocyclohexanediylbis (nitrilo-methylidyne)]bis (5-dimethyl-amino]phenol, have been studied. The two polymorphs concomitantly crystallized by vapour diffusion of solvent. The first polymorph (I) crystallized as a racemate in the centrosymmetric tetragonal $I4_1/a$ space group. The second polymorph (II) crystallized in the chiral orthorhombic space group $P2_12_12_1$. The chiral conformers of symmetrical *cis*-1,2-disubstituted cyclohexane molecules cannot be resolved in the liquid or gas phases, due to the rapid ring inversion. In the present study, the two chiral conformers are present in crystals of polymorph I, whereas, only one chiral conformer is present in crystals of polymorph II. Crystal structure analysis indicated that the formation of two different polymorphs of [Co(II)(L)] complex can be rationalized based on C—H···Co anagostic interactions. Density Functional Theory (DFT) calculations indicated that C—H···Co interactions are due to HOMO-LUMO interactions.

1. Introduction

Solid state polymorphism refers to different arrangements of crystalline species inside crystalline lattices. Different polymorphs, especially conformational polymorphs, are expected to have different physical properties [1–3] including solubility, density, optical, magnetic … etc. Variation in solubility caused by different polymorphs is important in pharmacology as it leads to different pharmacokinetics. A well-known example of the effect of polymorphism on solubility is the drug Ritonavir which is used to treat Acquired Immunodeficiency Syndrome (AIDS). The formation of a new stable conformational polymorph of Ritonavir with reduced solubility leads to reduced bioavailability, which required reformulation of the drug [2].

The polymorphism phenomenon is not very well understood yet. The general methodology of studying polymorphism is either by preparing different polymorphs serendipitously or intentionally and then rationalizing the supramolecular structure of the different polymorphs using the weak noncovalent interactions connecting the crystalline units or conformational differences [4]. So far, there is no guaranteed method to obtain different polymorphs [3,5]. However, there is significant progress in the area of crystal structure prediction [6]. Different crystallization conditions may results in the formation of different polymorphs including solvent of crystallization [7–9], temperature [10,11], pH [12], pressure [13,14] and the use of auxiliary molecules [7].

The arrangement of different conformers leads to the formation of conformational polymorphs [1], whereas different arrangements of a conformer result in the formation of packing polymorphs. Thirty-six percent of the reported polymorphs in the Cambridge Structural Database is conformational polymorphs [1]. Symmetrical *cis*-1,2-disubstituted cyclohexane molecules exist as two equivalent non-separable conformers in the liquid and gas phases due to the rapid inversion of the cyclohexane ring. As shown in Fig. 1, A and B′ are identical enantiomers and so are B and A'.

Crystallization of symmetrical *cis*-1,2-disubstituted cyclohexane as pure enantiomer is rare, only nine organic and one organometallic examples are known [15–23]. None of these ten examples crystallizes as different polymorphs. In this paper, we report the synthesis and crystal structure of two polymorphs of [Co(II)(L)] where H_2L = 2,2'-[*cis*-1,2-diamino-cyclohexanediylbis (nitrilo-methylidyne)]bis (5-dimethyl-amino]phenol (Fig. 2). Polymorph (I) crystallizes as a racemate in the centrosymmetric space group $I4_1/a$ space group, while polymorph (II) crystalizes as pure enantiomers in the chiral space group $P2_12_12_1$. The two polymorphs crystallize concomitantly from the same solution with approximately 1:1 ratio

* Corresponding author.
E-mail address: fawwadi@yahoo.com (F.F. Awwadi).

https://doi.org/10.1016/j.molstruc.2017.10.073
0022-2860/

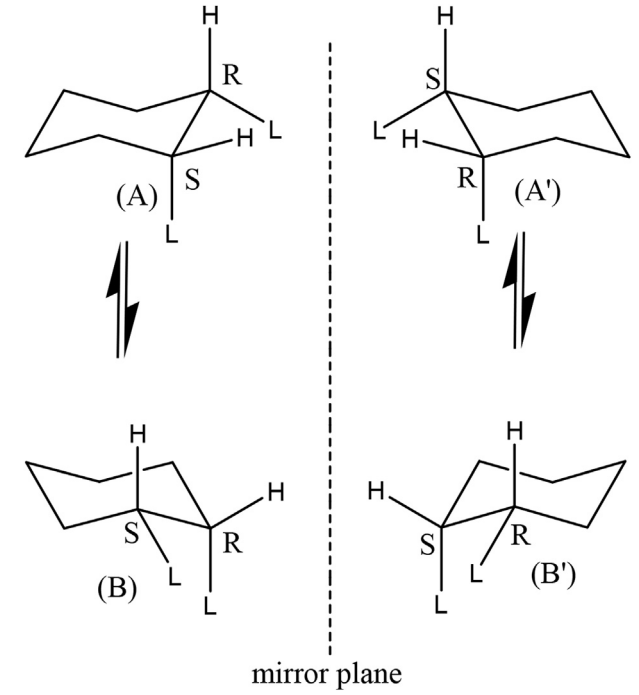

Fig. 1. The enantiomeric conformers of symmetrical *cis*-1,2- disubstituted cyclohexane molecules. The assignment of R and S configuration for the two chiral centers in (A) is arbitrary.

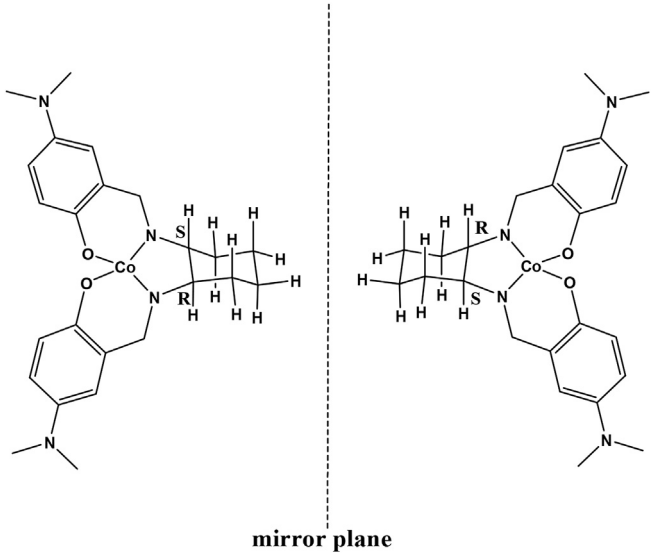

Fig. 2. The two chiral conformers of [Co(II)(L)]. The assignment of R and S configuration for the two chiral centers in the left image is arbitrary.

as inspected under microscopy. To our knowledge, these two polymorphs are the first examples in the literature in which symmetrical *cis*-1,2-disubstituted cyclohexane complexes crystallizes as a racemate (Polymorph I) and pure enantiomer (Polymorph II).

2. Experimental

2.1. Preparation of 4-N,N-dimethylamino-2-hydroxybenzaldehyde

The compound was prepared following the literature procedure with some modifications [24]. The Vilsmeier Haack adduct was prepared by addition of $POCl_3$ (15.0 mL, 0.16 mol) dropwise to dry DMF (30 mL) at 0 °C, and the mixture was then stirred for 30 min at the same temperature. To the adduct, a solution of 3-(*N*,*N*-dimethylamino)phenol (11.0 g, 80.3 mmol) in dry DMF (23 mL) was added dropwise at 0 °C. The reaction mixture was slowly warmed to room temperature, stirred for 4 h, and then heated at 85–90 °C for 30 min. The reaction mixture was allowed to cool to room temperature and kept at that temperature with stirring overnight. It was then poured into crushed ice and neutralized with saturated aqueous solution of Na_2CO_3 (120 mL). The precipitate was filtered off, washed with water and dried in a vacuum oven at 25 °C for 4 h. Yield: 9.00 g (68%), m.p. 78–79 °C (lit. 80.5–81 °C). The compound was used without further purification. ^{1}H NMR (500 MHz, $CDCl_3$) (Fig. S1-S3): δ = 11.56 (1H, s, OH), 9.47 (1H, s, CHO), 7.24 (1H, d, *J* = 9 Hz, H-6), 6.24 (1H, dd, *J* = 9, 2.1 Hz, H-5), 6.03 (1H, d, *J* = 2.1 Hz, H-3), 3.02 (6H, s, CH_3); ^{13}C NMR (125 MHz, $CDCl_3$) (Fig. S4): δ = 192.4, 164.1, 156.2, 135.2, 111.7, 104.6, 97.2, 40.1. FT-IR: νCO = 1628 cm^{-1}.

2.2. Preparation of 2,2'-[cis-1,2-diaminocyclohexanediylbis(nitrilo-methylidyne)]-bis(5-dimethyl-amino]phenol, (H_2L)

A solution of 4-(*N*,*N*-dimethylamino)-2-benzaldehyde (1.00 g, 6.05 mmol) in dry ethanol (25 mL) was introduced into a 150-mL two-necked round bottomed flask equipped with a dropping funnel, a condenser, a nitrogen inlet and connected to a bubbler. *cis*-1,2-Diaminocyclohexane (0.346 g, 3.03 mmol) in dry ethanol (20 mL) was added dropwise. After the addition was complete, the reaction mixture was refluxed for 2 h. The reaction mixture was allowed to cool to room temperature and the solid was filtered off and washed with ethanol (2 × 10 mL). The yellow product was dried in a vacuum oven at 50 °C for 4 h. Yield: 1.16 g (94%), m.p. 190–192 °C. 1H NMR (500 MHz, $CDCl_3$) (Fig. S5-S7).: δ = 13.93 (2H, s, OH), 8.07 (2H, s, CHO), 7.03 (2H, d, *J* = 8.2 Hz, H-6, H-6′), 6.18 (2H, dd, 8.2, 2.0 Hz, H-7,H-7′), 6.13 (s, 2H, H9,H9′), 3.55 (2H, m, H-1,H-1′), 3.00 (12H, s, CH_3), 1.56–1.97 (8H, m, cyclohexyl); ^{13}C NMR (125 MHz, $CDCl_3$) (Fig. S8): δ = 166.0, 162.4, 153.9, 132.7, 109.0, 103.4, 99.1, 67.4, 40.1, 30.4, 22.6. FT-IR: νC = N = 1614 cm^{-1}. Anal. Calcd for C_{24} H_{32} N_4 O_2: C, 70.56; H, 7.90; N, 13.71. Found: C, 70.17; H, 8.36; N, 13.75. HRMS ((+)-ESI): *m*/*z* = 409.25980 (calcd. 408.54 for C_{24} H_{33} N_4 O_2, $[M + H]^+$).

2.3. Preparation of the cobalt complex, [Co(II)(L)]

A solution of the Schiff base H_2L (0.500 g, 1.22 mmol) in dry methanol (25 mL) was introduced into a 150-mL two-necked round bottomed flask equipped with a dropping funnel, a condenser and a nitrogen inlet and connected to a bubbler. Cobalt acetate tetrahydrate (0.304 g, 1.22 mmol) in dry methanol (20 mL) was added dropwise. After the addition was completed, the dark-brown reaction mixture was refluxed for 4 h. It was then cooled to room temperature and the solid precipitate was collected and washed with small amount of methanol. The orange-red product was dried in a vacuum oven at 50 °C for 4 h. Yield: 88%, m.p. 275–280 °C (dec.). . FT-IR: νC = N = 1575 cm^{-1}. Suitable crystals for single x-ray analysis were obtained by a vapour diffusion method, using the combination CH_2Cl_2/diethyl ether with diffusion of diethyl ether vapour into dichloromethane solution.

2.4. Crystal structure determinations

The crystal structures of cobalt polymorphs (I) and (II) were determined at room temperature using 'Xcalibur, Eos'

Table 1
Summary of data collection and refinement parameters for two polymorphs of [Co(II)(L)] complex.

Crystal	Polymorph I	Polymorph II
Formula	C24 H30 Co N4 O2	C24 H30 Co N4 O2
M_r	465.45	465.45
ρ_{calc} (Mg/m^3)	1.427	1.378
Crystal system	Tetragonal	Orthorhombic
Space group	$I4_1/a$	$P2_12_12_1$
a (Å)	18.2420 (6)	9.0553 (10)
b (Å)	18.2420 (6)	11.790 (2)
c (Å)	26.0404 (11)	21.021 (2)
V (Å^3)	8665.5 (5)	2244.3 (5)
CCDC	1556534	1556533
ind. Reflections	4400	4338
Data/restraints/parameters	4400/0/283	4338/0/284
R (int)	0.0406	0.0533
Z	16	4
Goodness of fit	1.045	1.024
Absolute structure parameter	–	0.001 (19)
R_1[a] [I > 2σ]	0.0464	0.0507
wR_2[b] [I > 2σ]	0.0932	0.0828
μ, mm^{-1}	0.821	0.793
Largest diff. peak and hole (e/Å^3)	0.382 and −0.229	0.545 and −0.307

[a] $R_1 = \Sigma||Fo| - |Fc||/|\Sigma |Fo|$.
[b] $wR_2 = \{ \Sigma w (Fo^2 - Fc^2)^2/\Sigma w (Fo^2)^2\}^{1/2}$.

diffractometer (Mo Kα radiation, λ = 0.7107 Å). Data were acquired and processed to give *hkl* files using CrysAlisPro software [25]. A preliminary solution was obtained using Olex2 program [26], then the structure solution and refinements were finished using SHELXTL program package [27]. Atoms other than hydrogen were refined anisotropically, hydrogen atoms were placed in the calculated positions using a riding model. Data collection parameters and refinement results are given in Table 1.

2.5. Theoretical calculations

Gaussian 09 was used to optimize the molecular structure of the [Co(II)(L)] complex on the (DFT/UB3LYP) level, (DFT = Density Functional Theory and B3LYP = Becke, 3-parameter, Lee-Yang-Parr [28]. cc-pvdz basis set was assigned for all atoms except Co atom, lanl2dz basis set with pseudo potential was assigned for Co atom. The starting geometry was extracted from the crystal structure data.

3. Results and discussion

3.1. Synthesis

The ligand resulting from the condensation of 4-(*N*,*N*-dimethylamino)-2-hydroxybenzaldehyde with *trans*-diaminocyclohexane (2,2'-[*trans*-1,2-diaminocyclohexanediylbis (nitrilomethylidyne)]bis (5-dimethyl-amino]phenol) was briefly mentioned in only one report [21]. However, no reports were found on the preparation and characterization of the corresponding ligand with *cis*-1,2-diaminocyclohexane. This ligand was prepared by refluxing 4-*N*,*N*-dimethylamino-2-hydroxybenzaldehyde and *cis*-1,2-diaminocyclohexane in dry ethanol (Scheme 1). The condensation was confirmed by the appearance of the stretching band for νC = N at 1614 cm^{-1}. The ligand was fully characterized by elemental analysis, ^{1}H and ^{13}C NMR and mass spectrometry. The Schiff base formed behaves as a tetradentate ligand binding to the metal ion through the imine nitrogen atoms and phenolic oxygen atoms. Reaction of the ligand (H_2L) with cobalt (II) acetate in dry methanol results in the formation of [Co(II)(L)] complex which was confirmed by the appearance of the ligand-related peaks, which are slightly shifted in the IR spectrum of the complex. However, the peak at 1614 cm^{-1} assigned to νC = N in the ligand spectrum was significantly shifted to lower frequency (1575 cm^{-1}) in the complex due to cobalt bonding to the azomethine nitrogen. The complex was fully characterized by single crystal X-ray analysis (Fig. 3).

3.2. Crystallographic results

Crystals of [Co(II)(L)] were grown by gas diffusion of diethyl ether into a dichloromethane solution of the [Co(II)(L)] complex. Examination of the crystals of the [Co(II)(L)] complex under a microscope indicated the presence of two types of crystals which concomitantly crystallized, with an approximately 1:1 ratio; (a) dark red sword-shaped crystals (Fig. S9 left), henceforth polymorph

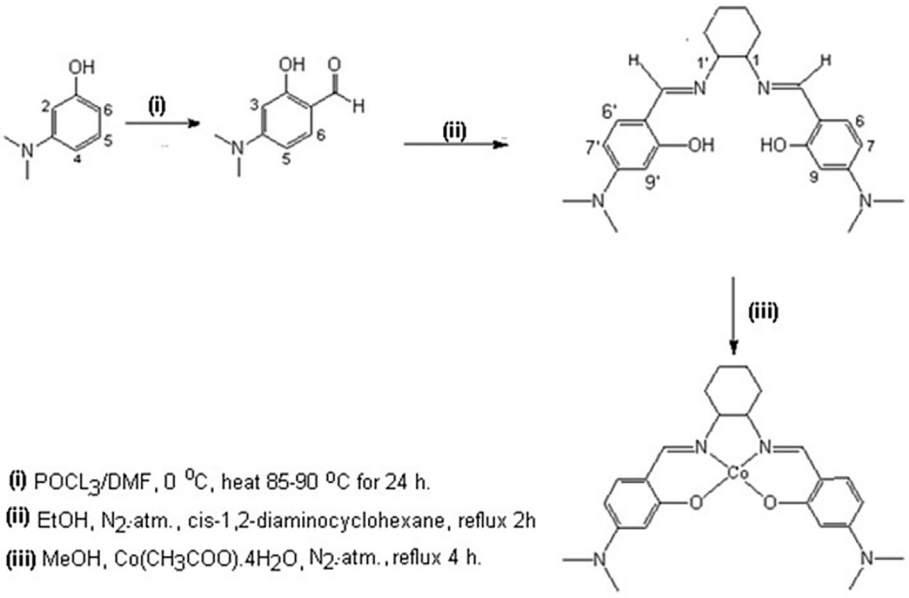

Scheme 1. Stepwise synthesis of [Co(II)(L)] complex.

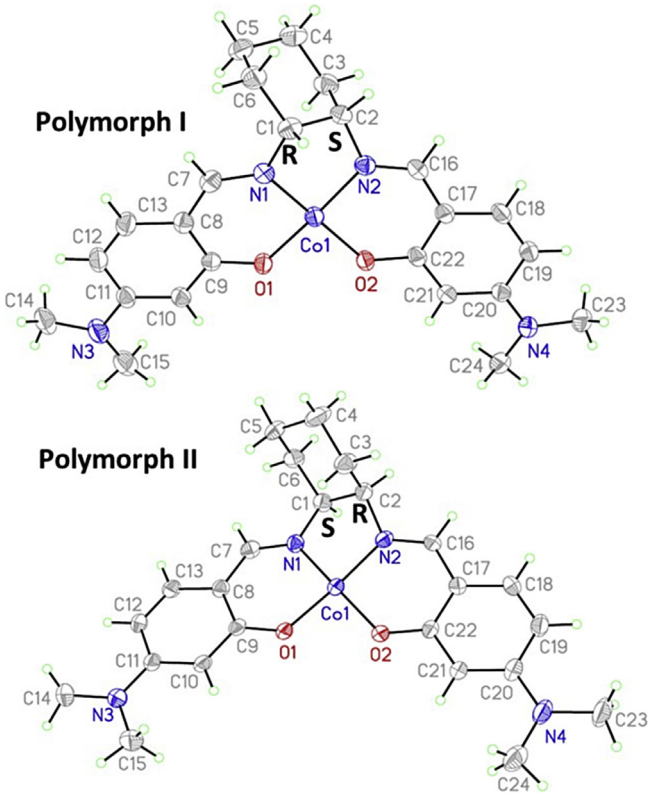

Fig. 3. Molecular structure of polymorph I (top) and polymorph II (bottom). Thermal ellipsoids are shown at 30% probability. In the case of Polymorph I, the structure represented corresponds to one enantiomer and the other enantiomer present in the structure is obtained by inversion.

I and, (b) lighter red parallelepiped-shaped crystals (Fig. S9 right), henceforth polymorph II. The sword-shaped crystals crystallize in the centrosymmetric tetragonal $I4_1/a$ space group, while, the parallelepiped crystals crystallized in the chiral orthorhombic chiral space group $P2_12_12_1$. The molecular structures of the two polymorphs are shown in Fig. 3.

The cyclohexane rings in both structures are in the chair conformation. X-ray analysis indicated that the molecules in the $I4_1/a$ phase are racemates with (50:50) of the two cyclohexane conformers, since $I4_1/a$ is a centrosymmetric space group, whereas they are pure enantiomers in the $P2_12_12_1$ phase as indicated by absolute structure parameters (Flack = 0.001 (19) (Table 2) and Hooft parameter = −0.024 (15)) [29,30]. The chiral center at C1 is of S configuration and that at C2 is of R configuration (Fig. 3) as determined by Platon software [31]. As expected, inverting the structure of Polymorph I does not change the refining parameters, whereas, upon inverting structure of Polymorph II the refining parameters [I > 2sigma(I)] rise from R1 = 0.0507 and w$R2$ = 0.0828 to R1 = 0.0617and w$R2$ = 0.1048 When the structure of both mirror images of polymorph I were overlaid on the structure of polymorph II (Fig. 4, only one structure of the mirror images of polymorph I is superimposable with the structure of polymorph II (Fig. 4).

The geometry around the metal center in the complexes is nearly square planar as indicated by the *cis* O1–Co–N1, O2–Co–N2, N1–Co–N2 and O1–Co–O2 angles and trans O1–Co–N2 and O2–Co–N1 angles; the average of the *cis* angles is 90.1°(range 83.6–94.1°) and the average of the trans angles is 174.7°(range 171.8–177.8°) (Fig. 3).it is noteworthy that the O–Co–N *cis* angles are larger than the O–Co–O or *N*–Co–O *cis* angles,

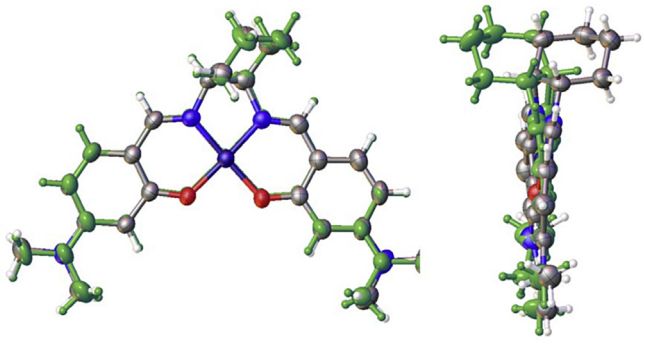

Fig. 4. Overlaid molecular structure of Polymorph II and the molecular structure of the two enantiomeric molecules found in the crystal structure of Polymorph I.

Table 2
Selected bond length (Å) and angles (°).

	Polymorph I	Polymorph II	Optimized
Co–O1	1.866 (2)	1.850 (3)	1.862
Co–O2	1.868 (2)	1.861 (2)	1.866
Co–N1	1.874 (2)	1.872 (3)	1.902
Co–N2	1.863 (2)	1.850 (4)	1.888
N1–C1	1.491 (4)	1.501 (5)	1.484
N2–C6	1.468 (4)	1.478 (4)	1.467
C1–C6	1.522 (4)	1.532 (5)	1.541
O (1)-Co(1)-N (2)	176.0 (1)	171.8 (1)	175.8
O (1)-Co(1)-O (2)	88.09 (8)	87.35 (10)	87.7
N (2)-Co(1)-O (2)	93.26 (10)	93.46 (12)	93.1
O (1)-Co(1)-N (1)	94.05 (10)	94.10 (12)	93.9
N (2)-Co(1)-N (1)	85.11 (11)	85.87 (14)	85.7
O (2)-Co(1)-N (1)	172.3 (1)	174.4 (1)	174.7
N (1)-C (1)-C (6)	104.9 (2)	104.5 (3)	105.8
N (2)-C (6)-C (1)	105.5 (2)	105.8 (3)	106.5
N (2)-C (6)-C (5)	110.3 (3)	109.6 (3)	110.6
N (1)-C (1)-C (2)	117.6 (3)	117.5 (3)	117.6
C (1)-C (6)-C (5)	112.5 (3)	112.5 (3)	112.0
C (3)-C (2)-C (1)	112.4 (3)	114.7 (4)	113.6
C (2)-C (3)-C (4)	110.2 (3)	110.9 (4)	110.6
C (4)-C (5)-C (6)	111.7 (3)	111.4 (4)	112.1
C (3)-C (4)-C (5)	110.7 (3)	109.9 (4)	110.9
C (6)-C (1)-C (2)	111.2 (3)	110.3 (4)	111.3
N1–C1–C6–N2	43.2 (3)	42.6 (4)	42.9
C2–C1–C6–C5	50.9 (4)	50.0 (5)	50.7

Table 3
C–H···Co anagostic interaction distances (Å) and angles (°). These interactions are depicted in Fig. 6.

Polymorph I		Polymorph II	
H24C···Co1	2.970	H1···Co1	2.829
C24···Co1	3.315	C1···Co1	3.665
C24–H24C···Co1	103	C1–H1···Co1	144
H24A … Co1	2.939	H5A … Co1	3.199
C24···Co1	3.315	C5···Co1	3.951
C24–H24A … Co1	105	C5–H5A … Co1	136

Table 4
C–H···O interaction distances (Å) and angles (°).These interactions are depicted in Fig. 7.

Polymorph I		Polymorph II	
H2B···O	2.628	H6···O1	2.445
C2···O1	3.566	C6···O1	3.339
C2–H2B···O1	163	C6–H6···O1	152
		H15B···O1	2.459
		C15 ··· O1	3.153
		C15–H15B···O1	129

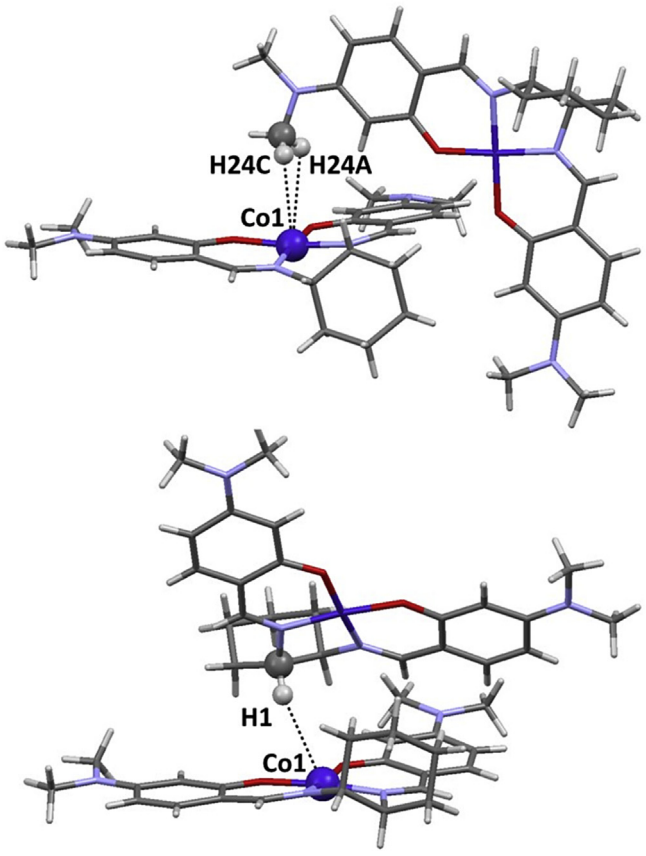

Fig. 5. Anagostic interactions in Polymorph I (top) and Polymorph II(bottom). The distances and angles of these interactions are listed in Tables 4 and 5

which is due to the fact that O–Co–N *cis* angles are part of a six membered ring, while *N*–Co–N *cis* angle is part of a five membered ring. Also, the mean deviations of atoms Co1, N1, N2, O1, O2 from the coordination planes are 0.079 and 0.090 Å for polymorph I and polymorph II, respectively. Selected bond distances and angles are given in Table 3.

The ligand has the same geometry in the two complex structures as indicated by the bond distances and angles (Table 2), although there are some small differences. The dimethylamine groups are closer to planar in Polymorph II than in Polymorph I, the mean deviations from the N2, C11, C14 and C15 plane are 0.068 and 0.008 for Polymorph I and Polymorph II, the corresponding deviations from N4, C20, C23, C24 are 0.038 and 0.010.

The supramolecular structure of the two Polymorphs is mainly developed based on the intermolecular interactions C–H···Co and C–H···O. The data summarizing these interactions are listed in Tables 3 and 4. The C–H···Co interactions exist in both structures (Fig. 5 and Table 4). The C–H···Co interactions collaborate with the C–H···O and C–H … π interactions to form chain structures in both complexes (Fig. 6); these chains run parallel to the c-axis in Polymorph I and parallel to the *a*-axis in the Polymorph II (Fig. 6).

In the cobalt polymorphs under investigation, C–H···Co interactions play a significant role in the formation of different polymorphs and hence chiral separation. Using the intermolecular forces in chiral separation has been reported in the literature [3]. The interaction of C–H with metal centers (C–H … M) is classified into two types; agostic and anagostic interactions [32,33]. The reported C–H···Co interactions in the two polymorphs are considered anagostic interactions since the H···Co distance is relatively long (avg. = 2.984 Å; range = 2.8299–3.199 Å, Table 3).

The crystallization of racemates in crystals of Polymorph I, but pure enantiomer molecules in crystals of Polymorph II can also be rationalized using C–H … M anagostic interactions. The interaction

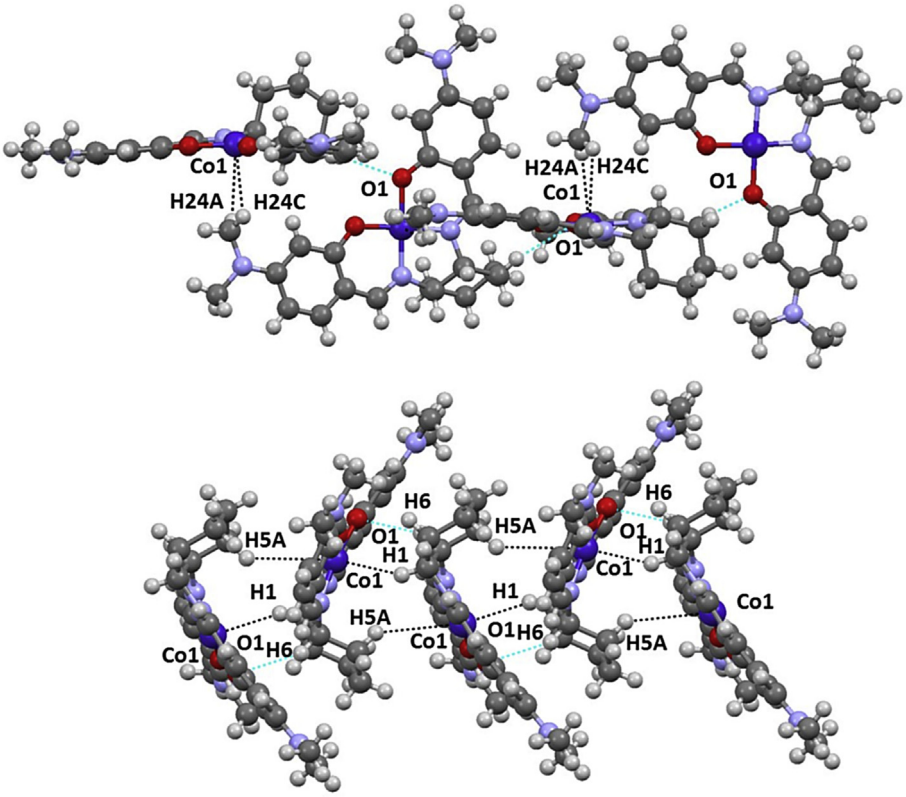

Fig. 6. Illustration of chain structure of polymorph I (top) and polymorph II (bottom). C–H···Co and C–H···O are represented by black and blue dotted lines. (For interpretation of the references to colour in this figure legend, the reader is referred to the web version of this article.)

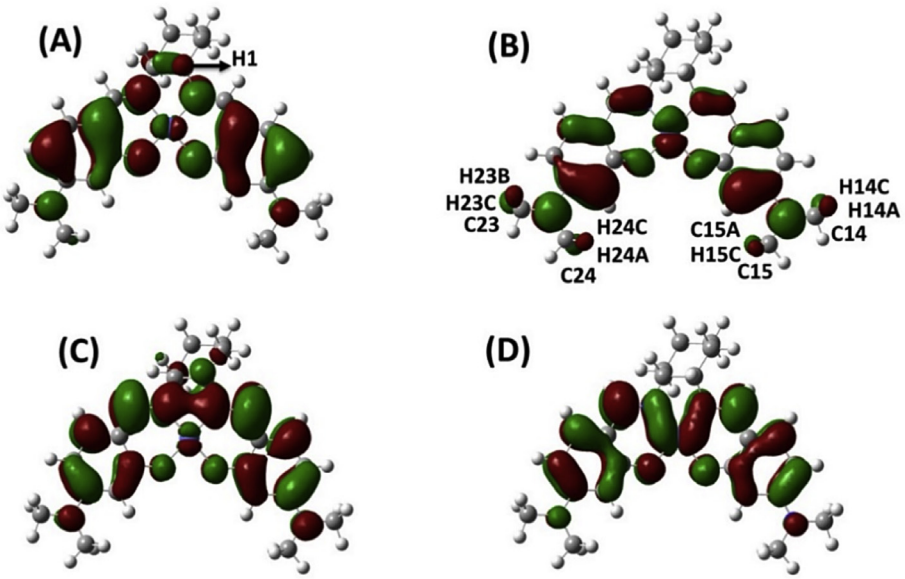

Fig. 7. Frontier orbitals of the optimized Co-complex; (A) HOMO-α, (B) HOMO-β, (C) LUMO-α and (D) LUMO-β. Isodensity is set to 0.02.

of the H1 atom (part of cyclohexane ring) with the Co atom of a different molecule restricts the ring flipping, indeed, only one enantiomer can enter the crystal. In contrast, no restrictions are imposed on the ring flipping in Polymorph I since hydrogen atoms (H24A and H22C) are involved in the anagostic interactions, rather than H1 (Fig. 5).

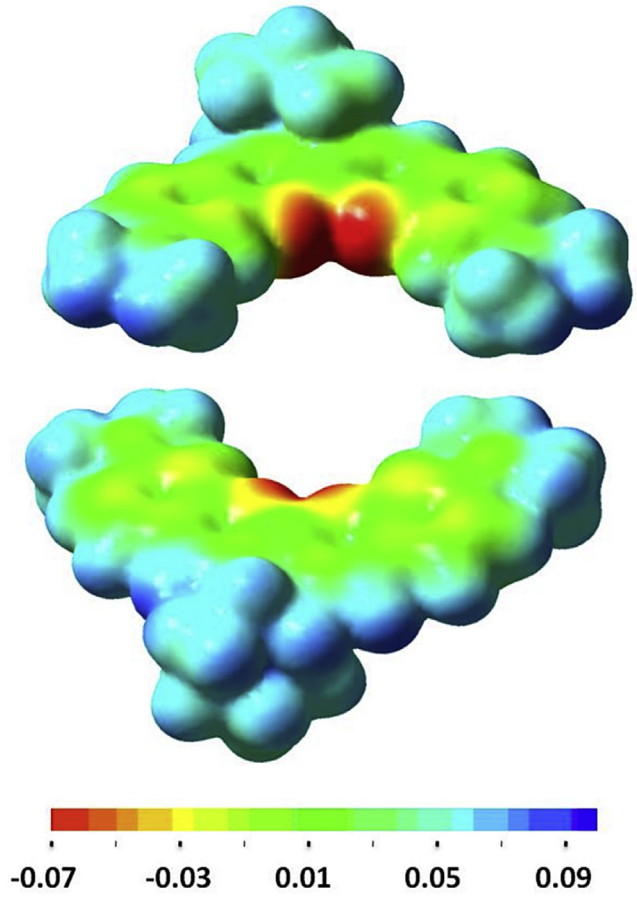

Fig. 8. Different views of the electrostatic potential of the [Co(II)(L)] complex. Contour isovalue is set to 0.005.

3.3. Theoretical results

The structure of the [Co(II)(L)] complex was optimized using the Gaussian (09) package at the DFT/UB3LYP level. The *Cc*-pvdz basis set was assigned for all atoms except the Co atom (lanl2dz). The crystallographic molecular structure was used as the starting geometry. Selected optimized bond lengths and angles are given in Table 2. The optimized bonds distances and angles are in excellent agreement with the experimental data. The average difference between the average experimental bond distances (average distances in the two polymorphs) in Table 2 and the corresponding calculated ones is 0.014 Å (range 0.002–0.03 Å), while the analogous difference in the listed angles in Table 2 is 0.5° (range 0.02–1.9°). The average of the experimental N1–C1–C2–N2 torsion angle and the calculated one are equal.

'Frontier Molecular orbitals and the electrostatic potential surface were calculated for the optimized [Co(II)(L)] complex. Molecular orbital analysis indicates that part of the HOMO's and LUMO's molecular orbitals are located on the metal center and this part of the molecular orbitals is perpendicular to the coordination plane. Also, the HOMO-α and HOMO-β span different atoms as shown in Fig. 7. It is noteworthy that the only involved hydrogen atom in the HOMO-α is the hydrogen atom attached to C1 (H1) (Fig. 7A), and

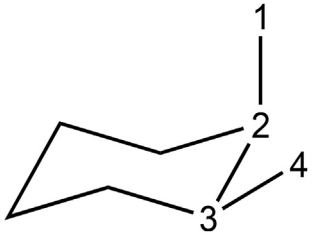

Fig. 9. Illustration of the *CSD* searching parameter. The C1–C2–C3–C4 angle is restricted to the range 0–60°.

Table 5
Reference codes and space groups of symmetrical *cis*-1,2-disubstituted cyclohexane molecules that crystallize in chiral space groups. The chemical structures of the these compounds are illustrated in Fig. 10.

Ref. code	Space group
AXOXIU [15]	$P2_1$
AXOXOA [15]	$P2_1$
BECVIQ [21]	$P2_12_12_1$
CEFSAJ [20]	$P1$
MOYFAH [18]	$P2_1$
DECDEW[a], [22]	$P21$
QOQTEV [19]	$P2_12_12_1$
TDOFEC10 [16]	$P2_1$
TEYGUZ [38]	$P2_1$
UZOVUB [23]	$C222_1$

[a] Two molecules in the asymmetric unit with a disordered cyclohexane ring in one of them.

hydrogen atoms attached to C14, C15, C23 and C24 are involved in the HOMO-β (H14A, H14C, H15A, H15C, H23B, H23C, H24A and H24C) (Fig. 7B). The electrostatic potential indicated positive electrostatic potential around hydrogen atoms (Fig. 8). The electrostatic potential is negative around the oxygen atoms. It is noteworthy that the potential is close to zero around the metal centers.

Molecular orbital analysis will be used to rationalize the anagostic interaction and electrostatic potential will be used to rationalize hydrogen bonding interactions. The C—H … M anagostic interactions are a result of HOMO-LUMO interactions between two adjacent molecules. The HOMO-LUMO interactions indicate that they are not due to electrostatic forces only [32]. The interaction has to be between two orbitals of different spin functions to satisfy the anti-symmetrization principle; the interaction has to be between HOMO-α and LUMO-β and *vice versa*. We have shown that H1 (Fig. 7A) is the only hydrogen atom involved in HOMO-α and (H14A,

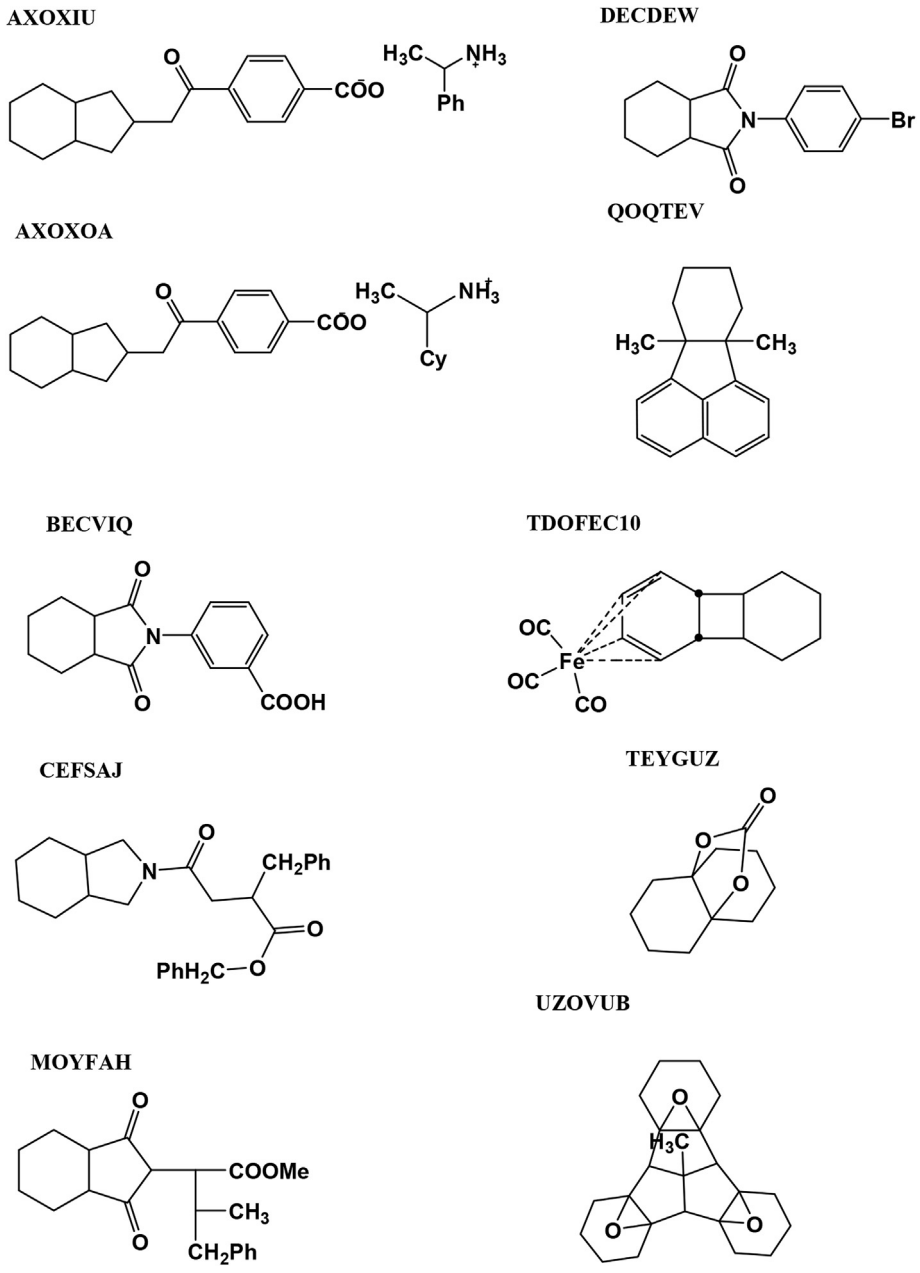

Fig. 10. Chemical structures of *cis*-1,2-disubstituted cyclohexane molecules that crystallize in chiral space groups (Ph = phenyl; Me = methyl; Cy = cyclohexyl).

H14C, H15A, H15C, H23B, H23C, H24A and H24C) hydrogen atoms are involved in the HOMO-β. Then, two possibilities of interactions arise; the H1 atom interacts with the metal center or (H14A, H14C, H15A, H15C, H23B, H23C, H24A and H24C) atoms interact with the metal center. The interactions of H24A and H24C (part of HOMO-β) with LUMO-α on the cobalt atom result in the formation of C–H … M interactions in the $I4_1/a$ phase (Figs. 7B and 5 (top)). The second possibility is the interaction of H1 (part of HOMO-α) with LUMO-β on the metal center. This is what is observed in Polymorph II (Figs. 7A and 5 (bottom)). This analysis indicates that the charge transfer from hydrogen to the metal center plays a significant role in these interactions. This is in agreement with the anagostic interactions that are associated with downfield chemical shift [32,34]. Calculated electrostatic potential has been used frequently to explain intermolecular interactions [35,36]. The hydrogen bond is mainly electrostatic in nature [37], therefore, the calculated electrostatic potential will be used to explain the hydrogen bonding interactions. The most negative potential values are around the oxygen atoms (Fig. 8). In contrast, the most positive values are around H atoms. Hence, C–H···O hydrogen bonding interactions are expected and observed (Fig. 6).

The polymorphs presented in this study are the first polymorphs reported in the literature in which one crystallizes as a racemate and the other crystallizes as a pure enantiomer of a symmetrical *cis*-1,2-disubstituted cyclohexane.The Cambridge Structural Data Base (CSD), version 5.37, July 2016, was searched for structures containing 1,2-disubstituted cyclohexane (Fig. 9). To limit our search to the *cis* 1,2-disubstituted isomers, the C1–C2–C3–C4 torsion angle was limited to 0–60° (Fig. 9). The search returned 1214 hits. Analysis of these hits for symmetrical *cis*-1,2-disubstituted cyclohexane indicated only 10 crystallize in chiral space groups (Table 5 and Fig. 10). All the chiral molecules reported in Table 5 are organic compounds except one organometallic compound (TDOFEC10) [16]. It is noteworthy that none of these examples exhibits polymorphs.

4. Conclusions

The two polymorphs presented in this paper are the first known examples in the literature in which a symmetrical *cis*-1,2-disubstituted cyclohexane derivative crystallizes as a racemate (in polymorph I) and as a pure enantiomer (in polymorph II). The formation of two different polymorphs as well as the chiral separation in polymorph II is due to C–H...Co anagostic interactions Symmetrical *cis*-1,2-disubstituted cyclohexane molecules exist as a mixture of two identical unisolable enantiomers in liquid and gas phases due to the rapid ring flipping. The [Co(II)(L)] complex crystallizes in two different polymorphs, the first one crystallize in the tetragonal $I4_1/a$ space group (Polymorph I), while, the second crystallizes in the chiral orthorhombic chiral space group $P2_12_12_1$ (Polymorph II). Analysis of the crystal structure of the two polymorphs indicates that the anagostic C–H···Co interactions can be used in chiral separation. The supramolecular structure of the two polymorphs can be rationalized using C–H···Co anagostic interactions. DFT/B3LYP calculations indicate that these interactions are a result of HOMO-LUMO interactions, which indicates that these interactions are not a result of electrostatic forces only.

Acknowledgements

FFA thanks Dr. Brendan Twamley of Trinity College of Dublin for searching Cambridge Structural Database for 1,2-disubstituted cyclohexane structure.

Appendix A. Supplementary data

Supplementary data related to this article can be found at https://doi.org/10.1016/j.molstruc.2017.10.073.

References

[1] A.J. Cruz-Cabeza, J. Bernstein, Conformational polymorphism, Chem. Rev. 114 (4) (2013) 2170–2191.
[2] J. Bauer, S. Spanton, R. Henry, J. Quick, W. Dziki, W. Porter, J. Morris, Ritonavir: an extraordinary example of conformational polymorphism, Pharm. Res. 18 (6) (2001) 859–866.
[3] B. Moulton, M.J. Zaworotko, From molecules to crystal engineering: supramolecular isomerism and polymorphism in network solids, Chem. Rev. 101 (6) (2001) 1629–1658.
[4] F.F. Awwadi, S.F. Haddad, Polymorphism in 2, 6-dimethylpyridinium tetrachlorocuprate (II): theoretical and crystallographic studies, J. Mol. Struct. 1020 (2012) 28–32.
[5] M.Y. Zhang, Z. Wang, T. Yang, Y. Zhang, X.F. Ma, Y.C. Sun, Z.W. Ouyang, M. Kurmoo, M.H. Zeng, Supramolecular interactions direct the formation of two structural polymorphs from one building unit in a one-pot synthesis, Chem. A Eur. J. 22 (39) (2016) 13900–13907.
[6] G.M. Day, C.H. Gorbitz, Introduction to the special issue on crystal structure prediction, Acta Crystallogr. Sect. B 72 (4) (2016) 435–436.
[7] V.Y. Torbeev, E. Shavit, I. Weissbuch, L. Leiserowitz, M. Lahav, Control of crystal polymorphism by tuning the structure of auxiliary molecules as nucleation inhibitors. The β-polymorph of glycine grown in aqueous solutions, Cryst. Growth & Des. 5 (6) (2005) 2190–2196.
[8] Y. Xu, Z. Xie, H. Zhang, F. Shen, Y. Ma, Conformational polymorphism of a twisted conjugated molecule: controllable torsional motion for crystal growth selectivity, CrystEngComm 18 (36) (2016) 6824–6829.
[9] I. Weissbuch, V.Y. Torbeev, L. Leiserowitz, M. Lahav, Solvent effect on crystal polymorphism: why addition of methanol or ethanol to aqueous solutions induces the precipitation of the least stable β form of glycine, Angew. Chem. Int. Ed. 44 (21) (2005) 3226–3229.
[10] F.F. Awwadi, R.D. Willett, B. Twamley, The aryl chlorine-halide ion synthon and its role in the control of the crystal structures of tetrahalocuprate (II) ions, Cryst. Growth & Des. 7 (4) (2007) 624–632.
[11] D.L. Cruickshank, C.H. Hendon, M.J. Verbeek, A. Walsh, C.C. Wilson, Polymorphism of the azobenzene dye compound methyl yellow, CrystEngComm 18 (19) (2016) 3456–3461.
[12] D. Gur, M. Pierantoni, N. Elool Dov, A. Hirsh, Y. Feldman, S. Weiner, L. Addadi, Guanine crystallization in aqueous solutions enables control over crystal size and polymorphism, Cryst. Grow. Des. 16 (9) (2016) 4975–4980.
[13] F.P. Fabbiani, D.R. Allan, W.I. David, A.J. Davidson, A.R. Lennie, S. Parsons, C.R. Pulham, J.E. Warren, High-pressure studies of pharmaceuticals: an exploration of the behavior of piracetam, Cryst. Growth & Des. 7 (6) (2007) 1115–1124.
[14] F.P. Fabbiani, D.R. Allan, S. Parsons, C.R. Pulham, An exploration of the polymorphism of piracetam using high pressure, CrystEngComm 7 (29) (2005) 179–186.
[15] S. Chen, B.O. Patrick, J.R. Scheffer, Enantioselective photochemical synthesis of a simple alkene via the solid state ionic chiral auxiliary approach, J. Org. Chem. 69 (8) (2004) 2711–2718.
[16] F. Cotton, V. Day, K. Hardcastle, Conformations of fused cycloalkanes in organometallic complexes: IV. The crystal and molecular structure of tricyclo-[6.4. 0.02. 7] dodeca-3, 5-dienetricarbonyliron, J. Organomet. Chem. 92 (3) (1975) 369–379.
[17] R. Eckrich, B. Neumann, H.-G. Stammler, D. Kuck, Stereoselective epoxidation of cyclohexa-anellated triquinacenes with iodine/silver (I) oxide as compared to m-chloroperbenzoic acid, J. Org. Chem. 61 (11) (1996) 3839–3843.
[18] J. Kimura, Y. Takada, T. Inayoshi, Y. Nakao, G. Goetz, W.Y. Yoshida, P.J. Scheuer, Kulokekahilide-1, a cytotoxic depsipeptide from the cephalaspidean mollusk philinopsis speciosa, J. Org. Chem. 67 (6) (2002) 1760–1767.
[19] M. Parvez, D.V. Simion, T.S. Sorensen, (6bR, 10aS)-6b, 10a-Dimethyl-10, 10a-dihydro-9H-fluoranthene, Acta Crystallogr. Sect. e. 57 (5) (2001) o441–o443.
[20] Z. Shang, L. Xu, L. Zheng, Y. Zhang, Benzyl 2-benzyl-4-[(3aS, 7aR)-2, 3, 3a, 4, 5, 6, 7, 7a-octahydro-1H-isoindol-2-yl]-4-oxobutanoate, Acta Crystallogr. Sect. E 68 (10) (2012) o2853.
[21] G. Smith, U.D. Wermuth, Hydrogen bonding in cyclic imides and amide carboxylic acid derivatives from the facile reaction of cis-cyclohexane-1,2-carboxylic anhydride with o- and p-anisidine and m- and p-aminobenzoic acids, Acta Crystallogr. Sect. C 68 (9) (2012) o327–o331.
[22] G. Smith, U.D. Wermuth, Cyclic imide and open-chain amide carboxylic acid derivatives from the facile reaction of cis-cyclohexane-1, 2-dicarboxylic anhydride with three substituted anilines, J. Chem. Crystallogr. 42 (10) (2012) 1029–1035.
[23] G. Mehta, S. Sen, Interesting modes of self-assembly of achiral 12-Oxo-11,13-dioxa[4.4.3]propellanes in a noncentrosymmetric environment, Cryst. Growth & Des. 11 (9) (2011) 3721–3724.
[24] R. Flašík, H. Stankovičová, A. Gáplovský, J. Donovalová, Synthesis and study of novel coumarin derivatives potentially utilizable as memory media, Molecules 14 (12) (2009) 4838–4848.

[25] CrysAlisPro, Agilent Technologies, Version 1.171.35.11 (Release 16–05–2011 CrysAlis171.NET) (Compiled May 16 2011, 17:55:39).
[26] O.V. Dolomanov, L.J. Bourhis, R.J. Gildea, J.A.K. Howard, H. Puschmann, OLEX2: a complete structure solution, refinement and analysis program, J. Appl. Cryst. 42 (2009) 339–341.
[27] SHELXTL (XCIF, XL, XP, XPREP, XS), Bruker AXS Inc., Madison, WI, 2002, version 6.10. .
[28] M.J. Frisch, G.W. Trucks, H.B. Schlegel, G.E. Scuseria, M.A. Robb, J.R. Cheeseman, G. Scalmani, V. Barone, B. Mennucci, G.A. Petersson, H. Nakatsuji, M. Caricato, X. Li, H.P. Hratchian, A.F. Izmaylov, J. Bloino, G. Zheng, J.L. Sonnenberg, M. Hada, M. Ehara, K. Toyota, R. Fukuda, J. Hasegawa, M. Ishida, T. Nakajima, Y. Honda, O. Kitao, H. Nakai, T. Vreven, J.A. Montgomery Jr., J.E. Peralta, F. Ogliaro, M. Bearpark, J.J. Heyd, E. Brothers, K.N. Kudin, V.N. Staroverov, T. Keith, R. Kobayashi, J. Normand, K. Raghavachari, A. Rendell, J.C. Burant, S.S. Iyengar, J. Tomasi, M. Cossi, N. Rega, J.M. Millam, M. Klene, J.E. Knox, J.B. Cross, V. Bakken, C. Adamo, J. Jaramillo, R. Gomperts, R.E. Stratmann, O. Yazyev, A.J. Austin, R. Cammi, C. Pomelli, J.W. Ochterski, R.L. Martin, K. Morokuma, V.G. Zakrzewski, G.A. Voth, P. Salvador, J.J. Dannenberg, S. Dapprich, A.D. Daniels, O. Farkas, J.B. Foresman, J.V. Ortiz, J. Cioslowski, D.J. Fox, Gaussian 09, Revision B.01, Gaussian, Inc., Wallingford CT, 2010.
[29] R.W. Hooft, L.H. Straver, A.L. Spek, Determination of absolute structure using Bayesian statistics on Bijvoet differences, J. Appl. Cryst. 41 (1) (2008) 96–103.
[30] S. Parsons, H.D. Flack, T. Wagner, Use of intensity quotients and differences in absolute structure refinement, Acta Crystallogr. Sect. B 69 (3) (2013) 249–259.
[31] A.L. Spek, Structure validation in chemical crystallography, Acta Crystallogr. Sect. D. 65 (2) (2009) 148–155.
[32] M. Brookhart, M.L. Green, G. Parkin, Agostic interactions in transition metal compounds, PNAS 104 (17) (2007) 6908.
[33] R. Angamuthu, L.L. Gelauff, M.A. Siegler, A.L. Spek, E. Bouwman, A molecular cage of nickel(ii) and copper(i): a [{Ni(L)2}2(CuI)6] cluster resembling the active site of nickel-containing enzymes, Chem. Comm. (19) (2009) 2700–2702.
[34] A. Husain, S.A. Nami, S.P. Singh, M. Oves, K. Siddiqi, Anagostic interactions, revisiting the crystal structure of nickel dithiocarbamate complex and its antibacterial and antifungal studies, Polyhedron 30 (1) (2011) 33–40.
[35] F.F. Awwadi, R.D. Willett, K.A. Peterson, B. Twamley, The nature of halogen⋯halogen synthons: crystallographic and theoretical studies, Chem. A Eur. J. 12 (35) (2006) 8952–8960.
[36] C.B. Aakeröy, T.K. Wijethunga, J. Desper, M. Đaković, Electrostatic potential differences and halogen-bond selectivity, Cryst. Growth & Des. 16 (5) (2016) 2662–2670.
[37] C.B. Aakeröy, A.M. Beatty, Review: crystal engineering of hydrogen-bonded assemblies-a progress report, Aus. J. Chem. 54 (7) (2001) 409–421.
[38] R. Eckrich, B. Neumann, H.-G. Stammler, D. Kuck, Stereoselective epoxidation of cyclohexa-anellated triquinacenes with iodine/Silver (I) oxide as compared to m-chloroperbenzoic acid, J. Org. Chem. 61 (11) (1996) 3839–3843.